

Recent Results with Delta-doped CCDs

Shouleh Nikzad, Todd J. Jones, Aimee Smith, Qiuming Yu, Paula J. Grunthaler, and S. Tom Elliott
Center for Space Microelectronics Technology
Jet Propulsion Laboratory, California Institute of Technology, Pasadena, CA 91109

Abstract

Delta-doped CCDs were developed at the Microdevices Laboratory at the Jet Propulsion Laboratory. Using molecular beam epitaxy, fully-processed thinned CCDs were modified by growing 2.5 nm of Boron-doped silicon on the back surface. Named delta-doped CCDs because of the sharply-spiked dopant profile in the thin epitaxial layer, these devices exhibited stable and uniform 100% internal quantum efficiency in the visible and ultraviolet regions of the spectrum. UV and charged-particle detection with delta-doped CCDs, and data from recent field measurements will be presented.

Introduction

Because of their large format, high resolution, low noise, and maturity of their development, CCDs are the detector of choice for many scientific (space or laboratory) applications. Standard frontside-illuminated CCDs do not respond in the UV because of short absorption of photons in this wavelength range. Untreated back-illuminated silicon CCDs have limited sensitivity to radiation (particles and photons) with short penetration depth, due to the surface depletion caused by the inherent positive charge in the native oxide. Because of surface depletion, internally-generated electrons are trapped near the irradiated surface and therefore cannot be transported to the detection circuitry. This deleterious surface potential can be eliminated by low-temperature molecular beam epitaxial (MBE) growth of a delta-doped layer on the Si surface. This effect has been demonstrated through achievement of 100% internal quantum efficiency for UV photons detected with delta-doped CCDs.

Processing of delta-doped CCDs was described previously.^{1,2} A 2.5 nm delta-doped Si layer is grown on the back surface of thinned, fully-processed CCDs at low-temperature. Delta-doped CCDs have been extensively tested and have shown 100% internal quantum efficiency in the ultraviolet and visible part of the spectrum indicating that the deleterious backside potential well responsible for the detector dead layer has been effectively eliminated. Because the delta-doped layer is incorporated directly into the silicon lattice, the modified CCDs are robust enough to withstand direct deposition of anti-reflection coatings for enhanced UV quantum efficiency.

Characterizing delta-doped CCDs using UV, FUV, and x ray sources

The quantum efficiency (QE) and stability of delta-doped CCDs in the UV and visible regions of the spectrum has been extensively measured. Figure 1 shows the typical quantum efficiency in the 250-700 nm region of the spectrum and the enhancement of the QE in the 300-400 nm region by direct deposition of single layer HfO₂.² The solid line in figure 1 is the silicon transmittance which represents 100% internal quantum or the maximum QE that can be obtained without addition of antireflection coatings. We have also measured the QE of delta-doped CCDs in the 121.6-310 nm region of the spectrum. It was shown in those measurements that the delta-doped CCD shows 100% internal QE throughout the entire 120-700 nm waveband.

Applications in astronomy require stable device performance. Figure 2 shows quantum efficiency data over a three-year period. No degradation of the device quantum efficiency was observed. The device stability with respect to history of illumination has also been examined. Increasing the exposure time by a factor of 100 and returning to the original exposure time yielded identical quantum efficiency for the delta-doped CCD, demonstrating that no quantum efficiency hysteresis exists in the device.

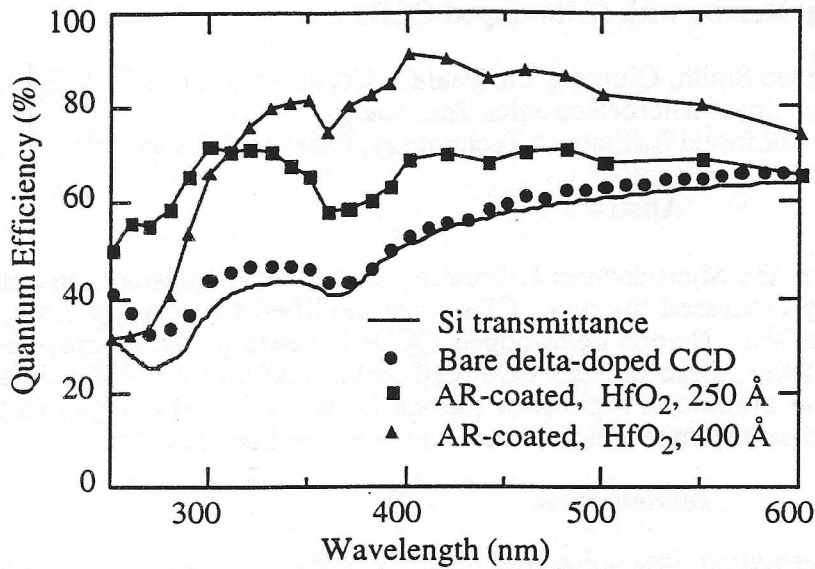


Figure 1. Quantum efficiency of a bare delta-doped CCD compared with solid line (Si transmittance) shows 100% internal QE. QE is enhanced by the addition of anti-reflection coatings optimized for the 270 nm to 400 nm regions (shown in squares and triangles).

X-ray measurements were performed on 1024x1024 pixel, 9 μm thick CCDs using Fe, Ti, Ca, K, Si, and Al targets. From these measurements, it was seen that very low-energy x rays, such as the aluminum K_{α} line, can be detected. In addition, measurements were performed using carbon and fluorine x rays. Because of their short absorption length, these x rays produce photo-electrons that are very vulnerable to backside recombination effects. These tests showed that no significant surface recombination was occurring.

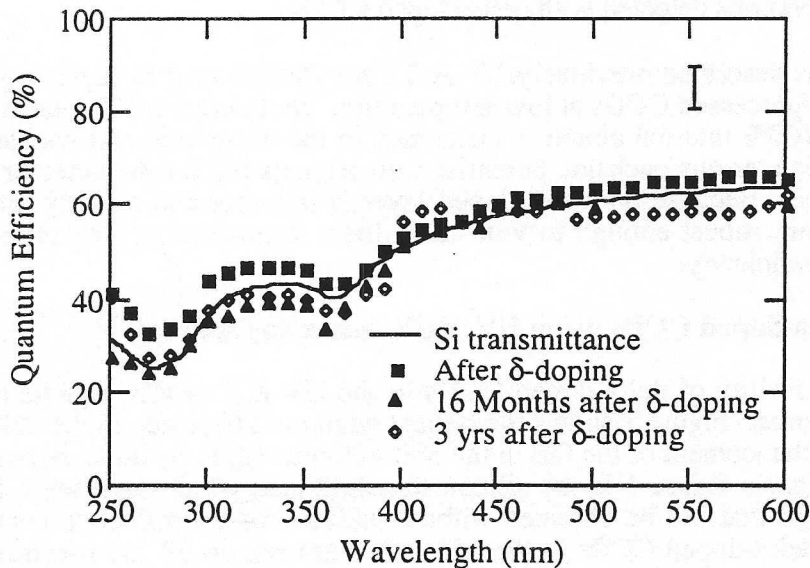


Figure 2. QE measured over a three-year period on the same delta-doped 512-by-512-pixel Reticon CCD. The CCD was stored unprotected in a laboratory environment. The error bars represent the accuracy ($\pm 5\%$) of the measurement systems used.

Low-energy particle detection with delta-doped CCDs

Imaging systems for low energy particles generally involve the use of microchannel plate electron multipliers followed by position sensitive solid state detectors, or phosphors and CCDs. These systems work well and can process up to 10^6 electrons/sec., however the spatial resolution of these compound systems is considerably less than that of a directly imaged CCD. Also, these systems have difficulties with gain stability and they require high voltages.

Similar to UV photons, low-energy particles deposit a significant fraction of their energy within a few nanometers of the surface, therefore, frontside-illuminated or untreated back-illuminated CCDs cannot detect low-energy particles. Quantum efficiency measurements in the UV indicate that electrons generated near the surface of delta-doped CCDs are detected efficiently and delta-doped CCDs are promising as imaging detectors of low-energy particles. We have extended the characterization of delta-doped CCDs to detection of electrons in the 50-1500 eV energy range using both a custom UHV chamber and a scanning electron microscope.^{3,4}

To gain an understanding of different aspects of low-energy electron response of delta-doped CCDs, we performed measurements using various electron sources and different device configurations. One set of measurements was performed in an SEM to take advantage of its highly-focused electron beam. The SEM apparatus was a JEOL, model JSM 6400, and the measurements were made with beam energies ranging between 200 eV and 1 keV. While it was not possible for modifications to be made to the SEM in order to accommodate the electronics necessary for collecting CCD images, performing photo-diode mode measurements was quite straightforward and informative. Another set of measurements was made in a UHV system in photo-diode mode. For this mode of measurement, each CCD in turn was mounted in plane with a Faraday cup and a phosphor screen onto a manipulator. Using the custom UHV system afforded the use of two different electron sources, one of very low energy and one of similar energies as used in the SEM measurements. The low-energy electron gun is a hot-filament cathode that produces electron energies of several 10 eV while generating a strong light background. Comparison was made between the observed response of the CCD and the response of the CCD with the electron beam magnetically deflected. Because of the strong CCD response to the background light, measurements with the hot filament electron gun beam are reported only qualitatively (50-200 eV). The UHV system further allowed for the later attachment of the electronics necessary for operating the CCD in imaging mode. This mode of operation allows for the observation of electron irradiation on operating parameters only apparent in imaging mode such as charge transfer efficiency (CTE), individual pixel response, and surface charging.

The CCDs used in these experiments were thinned, back-illuminated EG&G Reticon CCDs. All measurements were repeated with both delta-doped and untreated CCDs. In some of the measurements, direct comparisons of delta-doped CCDs with untreated CCDs were made on the same device, using a delta-doped CCD which included a controlled (untreated) region. The controlled region was provided on the back surface of the array by masking off a portion of the surface during the MBE growth. All devices were fully-characterized prior to the electron measurements using UV illumination.

Figure 3 shows the electron quantum efficiency of a delta-doped CCD plotted as a function of incident energy. Quantum efficiency was calculated by dividing the measured current from the CCD configured in photodiode mode to the measured electron beam current (measured by a Faraday cup), which is equivalent to the number of electron-hole pairs detected divided by the number of incident electrons. The measured quantum efficiency of the delta-doped CCD increases with increasing energy of the incident beam. The dependence of quantum efficiency on incident energy is due to the complicated interaction of electrons with silicon which results in the generation of multiple electron-hole pairs in the cascade initiated by each incident electron. A significant fraction of the incident energy is undetected, due to backscattering of incident electrons and other energy dissipation mechanisms (e.g., secondary and Auger electron emission). Multiple electron-hole pair production, also known in the literature as quantum yield, is also observed in the measured UV and x-ray response of delta-doped CCDs and other devices. Quantum yield greater than unity has been previously observed in backside-illuminated CCDs modified using the flashgate⁵ and ion implantation⁶ at electron energies greater than 1 keV.

The delta-doped CCD responds efficiently and reliably to low-energy electrons. Moreover, a delta-doped CCD responds with higher gain to low-energy electrons than other backside treated devices (e.g., twice that of a flashgate CCD). The untreated backside-thinned CCD showed a dramatically lower quantum efficiency than the delta-doped CCD (5% vs. 160% at 900 eV). The response of the untreated

CCD to electrons was unstable, decaying with a time constant on the order of 20 minutes at an incident electron energy of 1 keV. This decay was not reversible by a thermal anneal at $\sim 200^{\circ}\text{C}$.

In preliminary measurements conducted in our laboratory, we report the use of CCDs to image electrons. Images of 500 eV electrons with the delta-doped CCD show excellent qualitative similarity to UV images at 250 nm, with similar contrast between delta-doped and control regions of the CCD. Additional studies of electron imaging with the delta-doped CCD are under way.

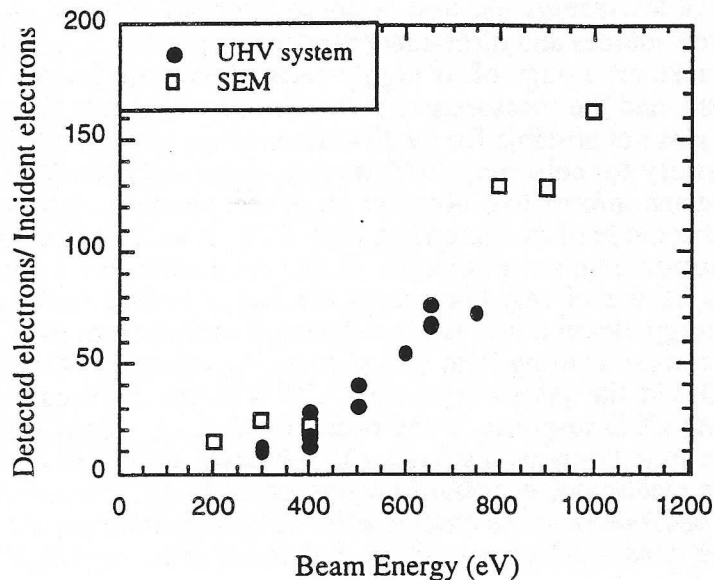


Figure 3 Ratio of detected electrons to incident electrons as a function of energy. The response of the CCD increases with increasing energy as result of multiple electron-hole pair generation.

Field observations and user feedback and evaluation

Delta-doped CCDs have been used recently in collaborations with a several scientists in a number of field observations. In collaboration with Caltech, a delta-doped CCD was used to image galaxies in the near UV at Caltech's Palomar observatory. In a sounding rocket experiment in collaboration with the University of Colorado, a delta-doped CCD was used as the detector in the spectrograph for ozone concentration measurements in the upper atmosphere. Use of delta-doped CCDs in very high precision photometry in collaboration with NASA Ames has been carried out showing that delta-doped CCDs have the dynamic range and stability necessary for high precision photometry.

Acknowledgments

The authors gratefully acknowledge the invaluable assistance of Drs. L.D. Bell, M.E. Hoenk, S. Manion, T. Van Zandt, Mr. W. Proniewicz, and Dr. M. Lesser (for antireflection coatings). The work presented in this paper was performed by the Center for Space Microelectronics Technology, Jet Propulsion Laboratory, California Institute of Technology, and was jointly sponsored by the National Aeronautics and Space Administration, Office of Space Science and the Caltech President's Fund.

References

1. M.E. Hoenk, P.J. Grunthaner, F.J. Grunthaner, M. Fattahi, H.-F. Tseng and R.W. Terhune, *Appl. Phys. Lett.*, **61** (9) 1084 (1992).
2. S. Nikzad, M.E. Hoenk, P.J. Grunthaner, R.W. Terhune, R. Wizenread, M. Fattahi, H.-F. Tseng, and F.J. Grunthaner. *Proc. of SPIE*, **2217**, *Surveillance Technologies III*, April 4-8, Orlando, Fl. (1994).
3. A. Smith, Q. Yu, S.T. Elliott, T.A. Tombrello, and S. Nikzad, *Proc. of the MRS*, **448**, Boston, Dec. 3, (1996).
4. S. Nikzad, A. Smith, T. Elliott, T.A. T.J. Jones, Tombrello, and Q. Yu, *Proc. SPIE*, **3019**, Feb. 11, San Jose, (1997).
5. T. Daud, J.R. Janesick, K. Evans, and T. Elliott, *Opt. Eng.*, **26** (8) 686 (1987).
6. D.G. Stearns and J.K. Wiedwald, *Rev. Sci. Instrum.* **60** (6)1095 (1989).